

SkeleVision: Towards Adversarial Resiliency of Person Tracking with Multi-Task Learning

Nilaksh Das, Sheng-Yun Peng, and Duen Horng Chau

Georgia Institute of Technology
{nilakshdas,speng65,polo}@gatech.edu

Abstract. Person tracking using computer vision techniques has wide ranging applications such as autonomous driving, home security and sports analytics. However, the growing threat of adversarial attacks raises serious concerns regarding the security and reliability of such techniques. In this work, we study the impact of multi-task learning (MTL) on the adversarial robustness of the widely used SiamRPN tracker, in the context of person tracking. Specifically, we investigate the effect of jointly learning with semantically analogous tasks of person tracking and human keypoint detection. We conduct extensive experiments with more powerful adversarial attacks that can be physically realizable, demonstrating the practical value of our approach. Our empirical study with simulated as well as real-world datasets reveals that training with MTL consistently makes it harder to attack the SiamRPN tracker, compared to typically training only on the single task of person tracking.

Keywords: person tracking, multi-task learning, adversarial robustness

1 Introduction

Person tracking is extensively used in various real-world use cases such as autonomous driving [3,50,53], intelligent video surveillance [4,54,1] and sports analytics [5,22,29]. However, vulnerabilities in the underlying techniques revealed by a growing body of adversarial ML research [42,14,35,6,11,46,20,49,7] seriously calls into question the trustworthiness of these techniques in critical use cases. While several methods have been proposed to mitigate threats from adversarial attacks in general [8,35,43,39,41], defense research in the tracking domain remains sparse [18]. This is especially true for the new generation of physically realizable attacks [6,11,46] that pose a greater threat to real-world applications.

In this work, we aim to investigate the robustness characteristics of the SiamRPN tracker [28], which is widely used in the tracking community. Specifically, our goal is to improve the tracking robustness to a physically realizable patch attack [46]. Such attacks are unbounded in the perceptual space and can be deployed in realistic scenarios, making them more harmful than imperceptible digital perturbation attacks. Figure 1 shows an example of such a physically realizable patch attack that blends in the background.

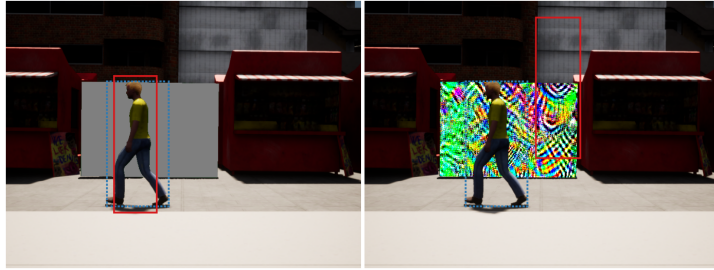


Fig. 1. Example of a physically realizable patch attack. The dashed blue box shows the ground-truth bounding box and the solid red box shows the bounding box predicted by SiamRPN. In the benign case (left), the tracker is able to correctly track the person whereas in the adversarial case (right) the tracker is fooled by the adversarial patch.

Multi-task learning (MTL) has recently been touted to improve adversarial robustness to imperceptible digital perturbation attacks for certain computer vision tasks [36,13]. However, it is unclear if these proposed methods translate to physically realizable attacks. Moreover, these methods have primarily been studied in the context of a single backbone branch with one-shot inference, whereas the Siamese architecture of the SiamRPN tracker involves multiple branched stages, posing interesting design considerations. In this work, we aim to address these research gaps by focusing on improving single-person tracking robustness.

As physically realizable attacks are unbounded in the perceptual space, they can create easily perceptible, but inconspicuous perturbations that fools a deep neural network into making incorrect predictions. However humans can ignore such perturbations by processing semantic knowledge of the real world. This calls for implicitly incorporating some inductive biases that supervise the neural network to learn semantic constraints that humans so instinctively interpret. To this effect, in this work we study the impact of MTL on robustness of person tracking with a semantically analogous task such as human keypoint detection.

Contributions

- **First Study of Tracking Robustness with MTL.** To the best of our knowledge, our work is the first to uncover the robustness gains from MTL in the context of person tracking for physically realizable attacks. Our code is made available at <https://github.com/nilakshdas/SkeleVision>.
- **Novel MTL Formulation for Tracking.** We augment the SiamRPN tracker for MTL by attaching a keypoint detection head to the template branch of the shared backbone while jointly training.
- **Extensive Evaluation.** We conduct extensive experiments to empirically evaluate the effectiveness of our MTL approach by varying attack parameters, network architecture, and MTL hyperparameters.
- **Discovery.** Our experiments with simulated and real-world datasets reveal that training with MTL consistently makes it harder to attack the SiamRPN tracker as compared to training only on the single task of person tracking.

2 Related Work

Since its inception with SiamFC [2], the Siamese architecture has been leveraged by multiple real-time object trackers including DSiam [15], SiamRPN [28], DaSiamRPN [63], SiamRPN++ [27], SiamAttn [55] and SiamMOT [40]. In this work, we experiment with SiamRPN as the target tracker since many other trackers share a similar network architecture as SiamRPN, and the properties of SiamRPN can be generalized to other such state-of-the-art trackers.

2.1 Multi-task Learning

MTL aims to learn multiple related tasks jointly to improve the generalization performance of all the tasks [61]. It has been applied to various computer vision tasks including image classification [34], image segmentation [36], depth estimation [31], and human keypoint detection [21].

MTL has also been introduced for the video object tracking task [25,23,24]. Zhang *et al.* [56,57,58] formulate the particle filter tracking as a structured MTL problem, where learning the representation of each particle is treated as an individual task. Wang *et al.* [45] show that joint training of natural language processing and object tracking can link the local and global search together, and lead to a better tracking accuracy. Multi-modal RGB-depth and RGB-infrared tracking also demonstrate that including the depth or infrared information in the tracking training process can improve the overall performances [51,62,59,60].

2.2 Adversarial Attacks

Machine learning model are easily fooled by adversarial attacks [9]. Adversarial attacks can be classified as digital perturbation attacks [42,14,35] and physically realizable attacks [6,11,46,49]. In the tracking community, multiple attacks have been proposed to fool the object tracker [20,7]. Fast attack network [30] attacks the Siamese network based trackers using a drift loss and embedded features. The attack proposed by Jia *et al.* [19] degrades the tracking accuracy through an IoU attack, which sequentially generates perturbations based on the predicted IoU scores. The attack requires ground-truth when performing the attack. Wiyatno and Xu [46] propose a method to generate an adversarial texture. The texture can lock the GOTURN tracker [16] when a tracking target moves in front of it.

2.3 Adversarial Defenses in Tracking

General defense methods for computer vision tasks include adversarial training [43], increasing labeled and unlabeled training data [39], decreasing the input dimensionality [41], and robust optimization procedures [52,48]. However, not many defense methods have been proposed to improve the tracking robustness under attack. Jia *et al.* [18] attempt to eliminate the effect of the adversarial perturbations via learning the patterns from the attacked images. Recently, MTL

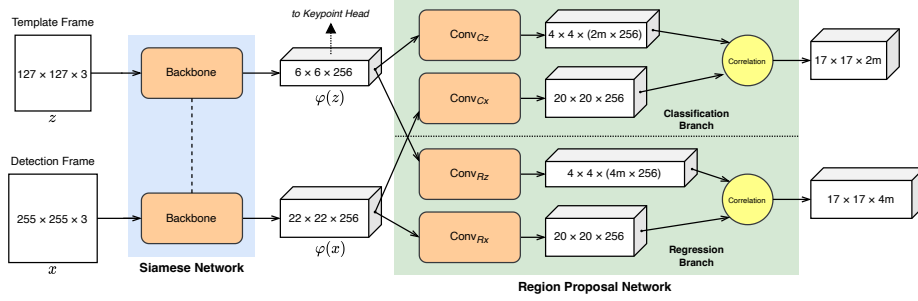


Fig. 2. Overview of the SiamRPN architecture for tracking. For multi-task learning, the output of the template branch is passed to a keypoint head for keypoint detection.

has been shown to improve the overall network robustness [13], especially in image segmentation [36] and text classification [33]. Our work is the first that studies MTL for person tracking with a physically realizable attack.

3 Preliminaries

The input to the tracker can be denoted as $\{x, z, \bar{y}_x, \bar{y}_z\}$, where x is the detection frame in which the subject is to be tracked, z is the template frame containing an exemplar representation of the subject, and respectively, \bar{y}_x and \bar{y}_z are the ground-truth bounding box coordinates within the corresponding frames.

3.1 Tracking with SiamRPN

In this work, we focus on the Siamese-RPN model (SiamRPN) [28], which is a widely used tracking framework based on the Siamese architecture. An overview of the SiamRPN architecture is shown in Figure 2. SiamRPN consists of a Siamese network for extracting features and a region proposal network (RPN), also referred to as the RPN head, for predicting bounding boxes.

The Siamese network has two branches: (1) the *template branch* which receives a template patch $z' = \Gamma(z, \bar{y}_z, s_z)$ as input; and (2) the *detection branch* which receives a detection patch $x' = \Gamma(x, \bar{y}_x, s_x)$ as input. Here, $\Gamma(\cdot)$ is simply a crop operation that ensures only a limited context of size s centered on the bounding box y is passed to the network [28]. The corresponding sizes s_z and s_x are shown in Figure 2. For notational convenience, we use z for z' and x for x' hereon. The two branches of the Siamese network use a shared backbone model such that inputs to both branches undergo the same transformation $\varphi(\cdot)$. Hence, we can denote the output feature maps of the Siamese network as $\varphi(z)$ and $\varphi(x)$ for the template and detection branches, respectively. In this work, we use the SiamRPN model with AlexNet backbone [26].

The RPN head can also be separated into two branches as shown in Figure 2. Considering m anchors distributed across the detection frame, the classification

branch predicts whether each respective anchor is a background or foreground anchor. Hence, the classification branch has $2m$ output channels corresponding to m anchors. The regression branch on the other hand predicts 4 box coordinate regression deltas [38] for each anchor, and therefore has $4m$ output channels.

While training, the classification and regression branches of the RPN head yield \mathcal{L}_{cls} and \mathcal{L}_{reg} respectively, where \mathcal{L}_{cls} is the cross-entropy loss and \mathcal{L}_{reg} is a smooth L_1 loss [28]. Finally, the total weighted loss optimized for is as follows:

$$\mathcal{L}_{TRK}(x, z, \bar{y}_x) = \lambda_C \mathcal{L}_{cls}(x, z, \bar{y}_x) + \lambda_R \mathcal{L}_{reg}(x, z, \bar{y}_x) \quad (1)$$

During inference, the network acts as a single-shot detector. Typically, a sequence of frames $\mathbf{x} = \{x_1, \dots, x_n\}$ is provided with the ground-truth bounding box coordinates \bar{y}_{x_1} of the first frame as input. Hence, the first frame x_1 becomes the template frame z used to compute the feature map $\varphi(z)$ once, which can be considered as detector parameters for predicting bounding box coordinates for input frames from the same sequence. We denote the predicted bounding box for an input frame as \hat{y}_x . As mentioned previously, SiamRPN crops the context centered on the ground-truth bounding box. For inference, the context region is determined by the predicted bounding box of the previous frame. Finally, the tracking performance is evaluated using a mean intersection-over-union (mIoU) metric of the predicted and ground-truth bounding boxes across all frames from all input sequences.

3.2 Multi-task Learning with Shared Backbone

To provide semantic regularization for tracking, we perform joint multi-task training by attaching a fully convolutional keypoint prediction head to the template branch of SiamRPN. Our hypothesis is that joint training with an additional task head attached to the shared backbone would encourage the backbone to learn more robust features [17] for facilitating multiple tasks. Since the shared backbone is also used during tracking inference, the learned robust features can make it harder for adversarial perturbations to fool the model. We select the task of human keypoint prediction for this purpose as it is more semantically analogous to the task of person tracking.

The keypoint head is attached to the template branch as it has a more focused context [28]. Therefore, the keypoint head receives $\varphi(z)$ as input. The keypoint head network consists of convolutional blocks followed by a transpose convolution operation that “upsamples” the intermediate feature map to an expanded size with number of output channels equaling the number of keypoints being predicted. Finally, bilinear interpolation is performed to match the size of the input frame. The resulting feature volume has a shape of $H \times W \times K$, where H and W are the height and width of the input frame respectively, and K is the number of keypoints. Hence, each position in the K -channel dimension corresponds to a keypoint logit score. Given the ground-truth keypoints \bar{k}_z , the binary cross-entropy loss is computed with respect to each position in the channel

dimension. We denote this as \mathcal{L}_{KPT} . For multi-task training, the total loss is a weighted sum:

$$\mathcal{L}_{MTL}(x, z, \bar{y}_x, \bar{k}_z) = \mathcal{L}_{TRK}(x, z, \bar{y}_x) + \lambda_K \mathcal{L}_{KPT}(z, \bar{k}_z) \quad (2)$$

The ground-truth keypoint annotation also consists of a visibility flag that allows us to suppress spurious loss from being backpropagated for keypoints that are occluded or not annotated.

3.3 Adversarial Attacks

Adversarial attacks introduce malicious perturbations to the input samples in order to confuse the tracker into making incorrect predictions. In this work, we use white-box untargeted attacks that aim to reduce the tracking performance by minimizing the mIoU metric. Adversarial attacks target a task loss, whereby the objective is to increase the loss by performing gradient ascent. Given the predicted and ground-truth bounding boxes \hat{y}_x and \bar{y}_x respectively, we use the L1-loss as the task loss as proposed in [46] for attacking an object tracker:

$$\mathcal{L}_{ADV}(\hat{y}_x, \bar{y}_x) = \|\hat{y}_x - \bar{y}_x\|_1 \quad (3)$$

Based on means of application of the adversarial perturbation and additional constraints placed on the perturbation strength, attacks can be further classified into two distinct types:

Digital Perturbation Attacks. These attacks introduce fine-grained pixel perturbations that are imperceptible to humans [42,14,35]. Digital perturbation attacks can manipulate any pixel of the input, but place imperceptibility constraints such that the adversarial output x_{adv} is within an l_p -ball of the benign input x_{ben} , *i.e.*, $\|x_{adv} - x_{ben}\|_p \leq \epsilon$. Such attacks, although having high efficacy, are considered to be physically non-realizable. This is due to the spatially unbounded granular pixel manipulation of the attack as well as the fact that a different perturbation is typically applied to each frame of a video sequence.

Physically Realizable Attacks. These attacks place constraints on the input space that can be manipulated by the attack [6,11,46,49]. In doing so, the adversarial perturbations can be contained within realistic objects in the physical world, such as a printed traffic sign [6] or a T-shirt [49]. As an attacker can completely control the form of the physical adversarial artifact, physically realizable attacks are unbounded in the perceptual space and place no constraints on the perturbation strength. In this work, we consider a physically realizable attack based on [46] that produces a background patch perturbation to fool an object tracker (Figure 1). It is an iterative attack that follows gradient ascent for the task loss described in Equation (3) by adding a perturbation to the input that is a product of the input gradient and a step size δ :

$$x^{(i)} = x^{(i-1)} + \delta \nabla_{x^{(i-1)}} \mathcal{L}_{ADV} \quad (4)$$

4 Experiment Setup

We perform extensive experiments and demonstrate that models trained with MTL are more resilient to adversarial attacks. The multi-task setting consists of jointly training a shared backbone for semantically related tasks such as person tracking and human keypoint detection (Section 4.1). We evaluate the tracking robustness on a state-of-the-art physically realizable adversarial attack for object trackers. We test our models on a photo-realistic simulated dataset as well as a real-world video dataset for person tracking (Section 4.4).

4.1 Architecture

For tracking, we leverage a SiamRPN model (Figure 2) with an AlexNet backbone and an RPN head as described in [28]. The inputs to the model are a template frame (127×127) and a detection frame (255×255), fed to the backbone network. Finally, the RPN head of the model produces classification and localization artifacts corresponding to $m = 5$ anchors for each spatial position. The anchors have aspect ratios of $\{0.33, 0.5, 1, 2, 3\}$ respectively.

A keypoint head is also attached to the template branch of the network, *i.e.*, the keypoint head receives the activation map with dimensions $6 \times 6 \times 256$ as input. We attach the keypoint head to the template branch as the template frame has a more focused context, and typically has only one subject in the frame, leading to more stable keypoint training. The base keypoint head has 2 convolutional blocks with $\{128, 64\}$ channels respectively. We also perform ablation experiments by increasing the depth of the keypoint head to 4 blocks with $\{128, 128, 64, 64\}$ channels respectively (Section 5.2). The convolutional blocks are followed by a transpose convolution block with 17 output channels, which is the same as the number of human keypoints represented in the MS COCO format [32]. Bilinear interpolation is performed on the output of the transpose convolution block to expand the spatial output dimensions, yielding an output with dimensions $127 \times 127 \times 17$. Hence each of the 17 channels correspond to spatial logit scores for the 17 keypoints.

4.2 Training Data

We found that there is a dearth of publicly available tracking datasets that support ad-hoc tasks for enabling multi-task learning. Hence, for our MTL training, we create a hybrid dataset that enables jointly training with person tracking and human keypoint detection. For human keypoint annotations, we leverage the MS COCO dataset [32] which contains more than $200k$ images and $250k$ person instances, each labeled with 17 human keypoints. The MS COCO dataset also annotates person bounding boxes that we use for the tracking scenario. As the MS COCO dataset consists of single images, there is no notion of temporal sequences in the input. Hence, for person tracking, we leverage data augmentation to differentiate the template and detection frames for the person instance annotation from the same image. Therefore, the MS COCO dataset



Fig. 3. Annotated training examples from the MS COCO (left) and LaSOT (right) datasets for person tracking. MS COCO has additional human keypoint annotations.

allows us to train both the RPN head and keypoint head jointly for person tracking and human keypoint detection. We use the defined train and val splits for training and validation. Additionally, we merge this data with the Large-scale Single Object Tracking (LaSOT) dataset [12]. Specifically, we extract all videos for the “*person*” class for training the person tracking network. This gives us 20 video sequences, of which we use the first 800 frames from each sequence for training and the subsequent 100 frames for the validation set. Hence, the combined hybrid dataset from MS COCO and LaSOT enables our multi-task training. Figure 3 shows 2 example frames from MS COCO and LaSOT datasets.

4.3 Multi-Task Training

For the multi-task training, we fine-tune a generally pre-trained SiamRPN object tracker jointly for the tasks of person tracking and human keypoint detection. As we are specifically interested in the impact of multi-task training, we use the same loss weights λ_C and λ_R as proposed in [28] for the tracking loss \mathcal{L}_{TRK} . We perform an extensive sweep of the MTL loss weight λ_K associated with the keypoint loss \mathcal{L}_{KPT} (Section 5.1). For the baseline, we perform single-task learning (STL) for person tracking by dropping the keypoint head and only fine-tuning the RPN head with the backbone, *i.e.*, the STL baseline has $\lambda_K = 0$. All STL and MTL models are trained with a learning rate of 8×10^{-4} that yields the best baseline tracking results as verified using a separate validation set. We also study the impact of pre-training the keypoint head separately before performing MTL (Section 5.3). For pre-training the keypoint head, we drop the RPN head and freeze the parameters of the backbone network. This ensures that the RPN head parameters are still compatible with the backbone after pre-training the keypoint head. The keypoint head is pre-trained with a learning rate of 10^{-3} . We train all models for 50 epochs and select the models with best validation performance over the epochs.

4.4 Evaluation

We evaluate our trained STL and MTL models for the tracking scenario using the mIoU metric between ground-truth and predicted bounding boxes, which is first averaged over all frames for a sequence, and finally averaged over all sequences.

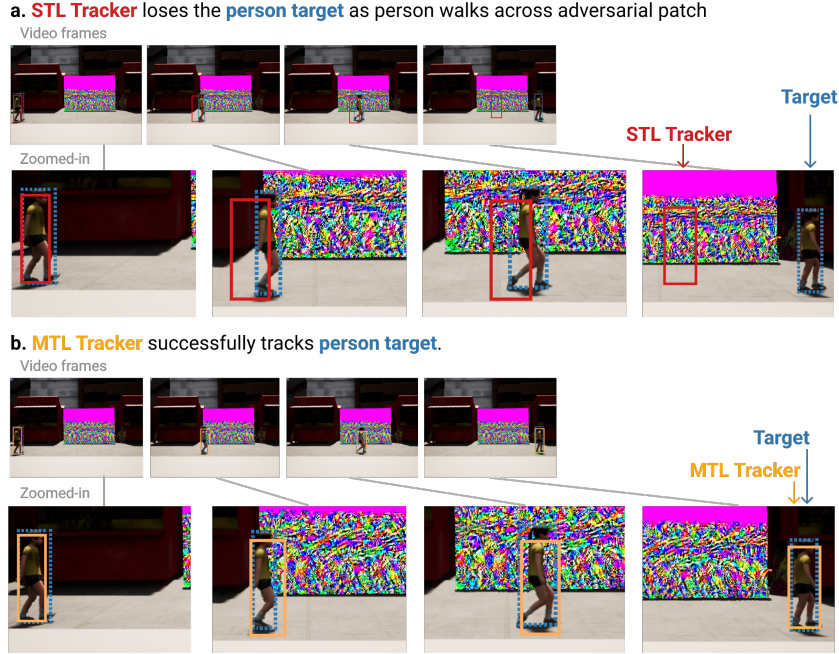


Fig. 4. Example video frames from the ARMORY-CARLA dataset showing static adversarial patches for (a) STL and (b) MTL for an attack with $\delta = 0.1$ and 10 steps. The patch is able to lock onto the STL tracker prediction (top), whereas the MTL tracker is consistently able to track the target (bottom).

For testing the adversarial robustness of person tracking in a practical scenario, we leverage a state-of-the-art physically realizable adversarial attack for object trackers [46]. The attack adds a static adversarial background patch to a given video sequence that targets the tracking task loss \mathcal{L}_{ADV} . At each iteration of the attack, gradient ascent is performed on the task loss as per Equation (4) with a step size δ . In order to observe the effect of varying the step size and attack iterations, we experiment with multiple values and report results for $\delta = \{0.1, 0.2\}$, which we found to have stronger adversarial effect on the tracking performance. The attack proposed in [46] has no imperceptibility constraints and is unbounded in the perceptual space, and can thus be considered an extremely effective adversarial attack. As the attack relies on the gradients of the task loss, we implement an end-to-end differentiable inference pipeline for the SiamRPN network using the Adversarial Robustness Toolbox (ART) framework [37].

We evaluate the adversarial robustness of STL and MTL models on 2 datasets: **ARMORY-CARLA**. This is a simulated photo-realistic person tracking dataset created using the CARLA simulator [10], provided by the ARMORY test bed [44] for adversarial ML research. We use the “dev” dataset split. The dataset consists of 20 videos of separate human sprites walking across the scene with various

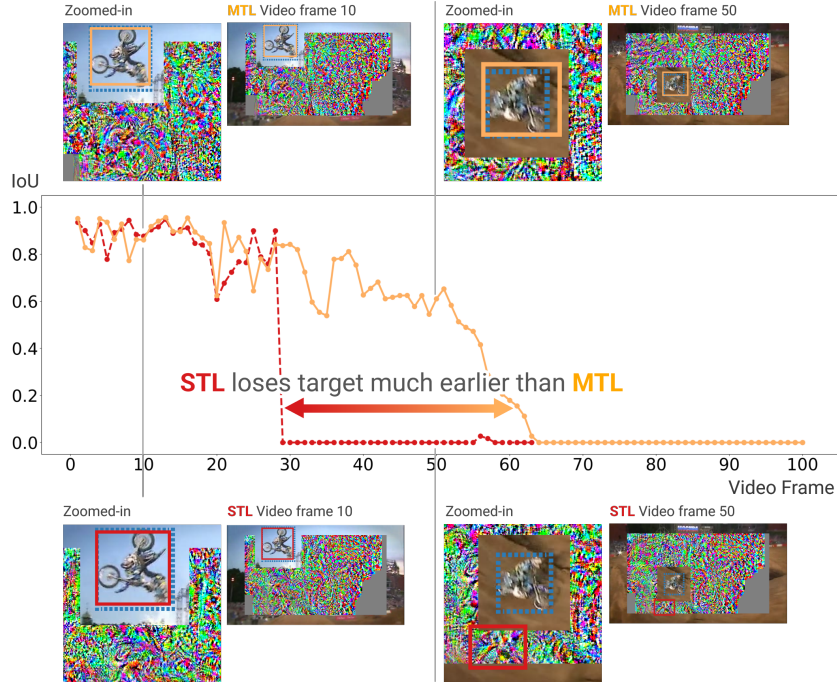


Fig. 5. Example video frames and the corresponding adversarial IoU charts for the video from the OTB2015-Person dataset showing the constructed static adversarial patches for STL (red) and MTL (orange) for an attack with $\delta = 0.1$ and 10 steps. The dashed blue box shows the ground-truth target. The attack misleads the STL tracker early, but struggles to mislead the MTL tracker until much later. The unperturbed gray regions in the patch are locations which are never predicted by the tracker.

background locations. Each video has an allocated patch in the background that can be adversarially perturbed to mimic a physically realizable attack for person tracking. The dataset also provides semantic segmentation annotations to ensure that only the patch pixels in the background are perturbed when a human sprite passes in front of the patch. Figure 4 shows example video frames from the dataset where this can be seen. We find that the SiamRPN person tracker, having been trained on real-world datasets, has a reasonably high mIoU for tracking the human sprites when there is no attack performed; thus qualifying the photo-realism of the simulated scenario.

OTB2015-Person. We use the Object Tracking Benchmark (OTB2015) [47] to test the robustness of MTL for person tracking on a real-world dataset. We extract all videos that correspond to the task of person tracking, which yields 38 videos that we call the OTB2015-Person split. As the dataset is intended for real-world tracking and is not readily amenable to implement physically realizable attacks, we digitally modify the videos for our attack to work. For each video, we overlay a static background patch that has a margin of 10% from

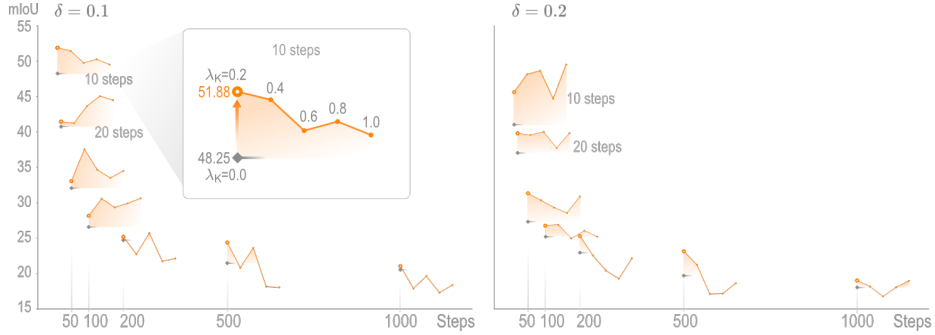


Fig. 6. A unified visualization of the adversarial mIoU results from Table 1 for the ARMORY-CARLA dataset with $\delta = 0.1$ (left) and $\delta = 0.2$ (right). The orange dots represent the MTL mIoU’s and the gray flat lines represent the STL baseline mIoU’s. We see that the hollow orange dots ($\lambda_K = 0.2$) are consistently above the STL baseline.

each edge, covering 64% of the total area that can be perturbed by the attack. Finally, for each frame of a video, we only uncover the region annotated by the ground-truth bounding box with a padding of 25 pixels on each side. Hence, the annotated subject is always completely visible to the tracker with a digitally perturbed adversarial patch boundary. Figure 5 shows example video frames with the static patch attack as described here. To ensure that the tracker gets a clean ground-truth template, we do not perturb the first frame. Since this implements an unbounded digital attack on inputs from the real-world perceptual space, the attack is much stronger than real-world physically realizable attacks. For computational tractability, we only attack the first 100 frames.

5 Results

Our experiments reveal that models trained with MTL consistently make it harder for an adversarial attack to succeed by making the shared backbone network learn robust MTL features. Given an iterative attack, higher number of iterations corresponds to increased attack difficulty and higher attacker cost. We report the mIoU for increasing attack steps from $\{10, 20, 50, 100, 200, 500, 1000\}$ for the ARMORY-CARLA dataset in Table 1. We also visually summarize these gains from the MTL approach for the ARMORY-CARLA dataset in Figure 6. For $\lambda_K = 1.0$, which is the base MTL setting, the MTL model improves upon the benign mIoU from 69.45 to 72.08. Additionally, the MTL model is more robust than the STL baseline up to 100 attack steps for $\delta = 0.1$ and 50 attack steps for $\delta = 0.2$. This implies the attack cost is higher for attacking an MTL model compared to its STL counterpart. The mIoU for increasing attack steps for the OTB2015-Person dataset are shown in Table 2. We observe a degradation in the benign MTL performance in this case, which may partly be attributed to the resolution mismatch between the high resolution training examples [32,12] from

Table 1. Adversarial mIoU results for ARMORY-CARLA dataset (\uparrow is better). Values highlighted in orange show the cases in which MTL is more robust than STL. MTL model with $\lambda_K = 0.2$ is consistently harder to attack than the STL model, and most often has the best performance. This table is also visualized in Figure 6 for clarity.

| | | STL | MTL | | | | |
|----------------|------|-------------------|-------------------|-------------------|-------------------|-------------------|-------------------|
| Steps | | $\lambda_K = 0.0$ | $\lambda_K = 0.2$ | $\lambda_K = 0.4$ | $\lambda_K = 0.6$ | $\lambda_K = 0.8$ | $\lambda_K = 1.0$ |
| <i>benign</i> | 0 | 69.45 | 69.59 | 69.46 | 69.70 | 72.20 | 72.08 |
| $\delta = 0.1$ | 10 | 48.25 | 51.88 | 51.44 | 49.74 | 50.24 | 49.50 |
| | 20 | 40.70 | 41.44 | 41.22 | 43.63 | 45.05 | 44.47 |
| | 50 | 32.07 | 33.04 | 37.54 | 34.63 | 33.49 | 34.49 |
| | 100 | 26.57 | 28.16 | 30.56 | 29.33 | 29.91 | 30.62 |
| | 200 | 24.72 | 25.19 | 22.73 | 25.70 | 21.73 | 22.12 |
| | 500 | 21.47 | 24.38 | 20.81 | 23.61 | 18.15 | 18.04 |
| | 1000 | 20.54 | 21.05 | 17.90 | 19.64 | 17.30 | 18.37 |
| $\delta = 0.2$ | 10 | 41.03 | 45.62 | 48.13 | 48.63 | 44.68 | 49.50 |
| | 20 | 37.04 | 39.78 | 39.57 | 40.00 | 37.72 | 39.81 |
| | 50 | 27.32 | 31.32 | 30.33 | 29.31 | 28.55 | 30.86 |
| | 100 | 25.24 | 26.76 | 26.89 | 24.95 | 26.03 | 25.21 |
| | 200 | 22.95 | 25.29 | 22.54 | 20.41 | 19.27 | 22.16 |
| | 500 | 19.71 | 23.13 | 21.23 | 17.11 | 17.18 | 18.63 |
| | 1000 | 18.04 | 19.02 | 18.16 | 16.77 | 18.04 | 18.97 |

orange = MTL > STL; gray = MTL \leq STL; bold = highest in row

MS COCO and LaSOT datasets, compared to lower resolution evaluation videos samples from the OTB2015 dataset. In the adversarial case, the base MTL model is more robust than STL baseline for up to 200 steps for $\delta = 0.1$. For $\delta = 0.2$, the base MTL model fails to show robustness for 20 steps, and slightly better robustness for other attack steps. We see further improvements in the adversarial resiliency for varying λ_K , discussed in Section 5.1.

5.1 Varying MTL Weight

We study the effect of varying the MTL weight λ_K , which controls the amount of keypoint loss \mathcal{L}_{KPT} that is backpropagated. We train separate models by enumerating $\lambda_K = \{0.2, 0.4, 0.6, 0.8, 1.0\}$, and perform adversarial patch attack on each model for multiple adversarial settings. The results for ARMORY-CARLA and OTB2015-Person are shown in Table 1 and Table 2 respectively. We find that for the given shallow keypoint head architecture ($\{128, 64\}$ channels), a lower value of λ_K is more optimal under adversarial attack. For both datasets, the MTL model with $\lambda_K = 0.2$ is consistently harder to attack than the STL model, and most often has the best performance for the corresponding adversarial setting. Since a shallow keypoint head has relatively lower learning capacity, a higher λ_K value will force the shared backbone to focus excessively on the keypoint detection task, causing deterioration in the robust MTL features learned for the

Table 2. Adversarial mIoU results for OTB2015-Person dataset (\uparrow is better). In most cases, MTL models are harder to attack compared to STL model, with $\lambda_K = 0.2$ being most robust to the attack across several attack steps and step sizes.

| | | STL | MTL | | | | |
|----------------|-----|-------------------|-------------------|-------------------|-------------------|-------------------|-------------------|
| Steps | | $\lambda_K = 0.0$ | $\lambda_K = 0.2$ | $\lambda_K = 0.4$ | $\lambda_K = 0.6$ | $\lambda_K = 0.8$ | $\lambda_K = 1.0$ |
| <i>benign</i> | 0 | 69.42 | 68.62 | 67.84 | 67.89 | 65.97 | 68.50 |
| $\delta = 0.1$ | 10 | 54.29 | 57.29 | 57.78 | 57.95 | 57.09 | 56.24 |
| | 20 | 52.62 | 55.45 | 55.68 | 55.56 | 53.01 | 52.68 |
| | 50 | 48.54 | 52.84 | 52.33 | 50.54 | 50.94 | 50.67 |
| | 100 | 44.92 | 52.45 | 48.54 | 48.63 | 48.77 | 48.25 |
| | 200 | 45.40 | 47.73 | 49.18 | 47.26 | 46.50 | 47.34 |
| $\delta = 0.2$ | 10 | 53.93 | 57.65 | 56.60 | 55.70 | 56.46 | 54.34 |
| | 20 | 53.57 | 55.21 | 56.16 | 56.08 | 54.46 | 52.86 |
| | 50 | 49.15 | 52.81 | 51.12 | 49.48 | 50.71 | 49.65 |
| | 100 | 47.27 | 52.72 | 49.74 | 48.13 | 49.87 | 47.81 |
| | 200 | 46.19 | 51.05 | 48.83 | 47.24 | 48.26 | 47.04 |

orange = MTL > STL; gray = MTL \leq STL; bold = highest in row

tracking task. From Table 1, although we observe better generalization for the MTL model with $\lambda_K = 1.0$ in the benign case (mIoU = 72.08), the adversarial robustness quickly gives away (at 100 steps for $\delta = 0.2$). Conversely, a lower value of $\lambda_K = 0.2$ offers the best trade-off for generalization and robustness.

5.2 Increasing Depth of Keypoint Head

Following the observations with a shallow keypoint head architecture, we also experiment with increasing the depth of the keypoint head from $\{128, 64\}$ channels to $\{128, 128, 64, 64\}$ channels, doubling the parameters of the keypoint head network. Table 3 shows the ablation results for the shallow and deep keypoint heads with the ARMORY-CARLA dataset for $\lambda_K = \{0.2, 1.0\}$ and $\delta = 0.1$. In this section we will focus on the “not pre-trained” results. The robustness of the MTL model degrades for $\lambda_K = 0.2$ when the model depth is increased, and is easier to attack compared to the STL model. However, the MTL model with deeper keypoint head has the best adversarial robustness for a higher $\lambda_K = 1.0$, even outperforming the MTL model with shallow keypoint head for $\lambda_K = 0.2$. As the deeper keypoint head has a relatively higher learning capacity, it can learn to detect keypoints with smaller changes to the feature space of the backbone network. Hence, a higher λ_K is required to adequately supervise the backbone in learning robust MTL features. Although we see a decline in the benign mIoU for increasing depth, the deep MTL model with $\lambda_K = 1.0$ has overall best robustness. On the other hand, the shallow MTL model with $\lambda_K = 0.2$ has better adversarial robustness than the STL model as well as better benign performance.

Table 3. Ablation study with the ARMORY-CARLA dataset for attack step size $\delta = 0.1$. We report the adversarial mIoU results (\uparrow is better).

| Steps | $\lambda_K = 0.0$ | $\lambda_K = 0.2$ | | | | $\lambda_K = 1.0$ | | | |
|-------|-------------------|----------------------------|-------|------------------------|-------|----------------------------|--------------|------------------------|-------|
| | (STL) | not pre-trained shallow | deep | pre-trained shallow | deep | not pre-trained shallow | deep | pre-trained shallow | deep |
| 0 | 69.45 | 69.59 | 66.85 | 69.62 | 69.36 | 72.08 | 67.28 | 64.14 | 69.40 |
| 10 | 48.25 | 51.88 | 45.28 | 47.05 | 48.70 | 49.50 | 55.46 | 49.91 | 49.77 |
| 20 | 40.70 | 41.44 | 38.54 | 39.94 | 40.47 | 44.47 | 47.44 | 43.10 | 42.55 |
| 50 | 32.07 | 33.04 | 31.71 | 34.11 | 35.28 | 34.49 | 36.52 | 36.31 | 32.96 |
| 100 | 26.57 | 28.16 | 27.21 | 31.33 | 32.04 | 30.62 | 30.07 | 32.14 | 31.60 |
| 200 | 24.72 | 25.19 | 24.15 | 25.67 | 25.34 | 22.12 | 26.53 | 25.16 | 24.77 |

orange = MTL > STL; gray = MTL \leq STL; bold = highest in row

5.3 Pre-training the Keypoint Head

As we start with a pre-trained SiamRPN model and an untrained keypoint head, we also study the impact of pre-training the keypoint head before performing MTL fine-tuning. Table 3 shows the results of this ablation study. We report the MTL performance with and without pre-training the keypoint head with the ARMORY-CARLA dataset for $\lambda_K = \{0.2, 1.0\}$ and $\delta = 0.1$. For the shallow keypoint head architecture, we see minor improvements in the MTL performance for a higher value of $\lambda_K = 1.0$, especially at higher number of attack steps. However, there is a sharp decrease in the benign performance (benign mIoU = 64.14). On the other hand, the deep keypoint head architecture shows relative improvement with pre-training for a lower value of $\lambda_K = 0.2$ (benign mIoU = 69.36). Overall, there is no significant advantage observed from pre-training the keypoint head. A pre-trained keypoint head would have lower potential to significantly modify the learned feature space of the shared backbone as it is already near the optima for the keypoint loss space.

6 Conclusion

We perform an extensive set of experiments with adversarial attacks for the task of person tracking to study the impact of multi-task learning. Our experiments on simulated and real-world datasets reveal that models trained with multi-task learning for the semantically analogous tasks of person tracking and human keypoint detection are more resilient to physically realizable adversarial attacks. Our work is the first to uncover the robustness gains from multi-task learning in the context of person tracking for physically realizable attacks. As the tracking use case has widely ranging real-world applications, the threat of adversarial attacks has equally severe implications. We hope our work triggers new research in this direction to further secure tracking models from adversarial attacks.

References

1. Ahmed, I., Jeon, G.: A real-time person tracking system based on siammask network for intelligent video surveillance. *Journal of Real-Time Image Processing* **18**(5), 1803–1814 (2021)
2. Bertinetto, L., Valmadre, J., Henriques, J.F., Vedaldi, A., Torr, P.H.: Fully-convolutional siamese networks for object tracking. In: *European conference on computer vision*. pp. 850–865. Springer (2016)
3. Bhattacharyya, A., Fritz, M., Schiele, B.: Long-term on-board prediction of people in traffic scenes under uncertainty. In: *Proceedings of the IEEE Conference on Computer Vision and Pattern Recognition*. pp. 4194–4202 (2018)
4. Bohush, R., Zakharava, I.: Robust person tracking algorithm based on convolutional neural network for indoor video surveillance systems. In: *International Conference on Pattern Recognition and Information Processing*. pp. 289–300. Springer (2019)
5. Bridgeman, L., Volino, M., Guillemaut, J.Y., Hilton, A.: Multi-person 3d pose estimation and tracking in sports. In: *Proceedings of the IEEE/CVF conference on computer vision and pattern recognition workshops*. pp. 0–0 (2019)
6. Chen, S.T., Cornelius, C., Martin, J., Chau, D.H.P.: Shapeshifter: Robust physical adversarial attack on Faster R-CNN object detector. In: *Joint European Conference on Machine Learning and Knowledge Discovery in Databases*. pp. 52–68. Springer (2018)
7. Chen, X., Fu, C., Zheng, F., Zhao, Y., Li, H., Luo, P., Qi, G.J.: A unified multi-scenario attacking network for visual object tracking. In: *Proceedings of the AAAI Conference on Artificial Intelligence*. vol. 35, pp. 1097–1104 (2021)
8. Cisse, M., Bojanowski, P., Grave, E., Dauphin, Y., Usunier, N.: Parseval networks: Improving robustness to adversarial examples. In: *International Conference on Machine Learning*. pp. 854–863. PMLR (2017)
9. Dong, Y., Liao, F., Pang, T., Su, H., Zhu, J., Hu, X., Li, J.: Boosting adversarial attacks with momentum. In: *Proceedings of the IEEE conference on computer vision and pattern recognition*. pp. 9185–9193 (2018)
10. Dosovitskiy, A., Ros, G., Codevilla, F., Lopez, A., Koltun, V.: CARLA: An open urban driving simulator. In: *Proceedings of the 1st Annual Conference on Robot Learning*. pp. 1–16 (2017)
11. Eykholt, K., Evtimov, I., Fernandes, E., Li, B., Rahmati, A., Xiao, C., Prakash, A., Kohno, T., Song, D.: Robust physical-world attacks on deep learning visual classification. In: *Proceedings of the IEEE conference on computer vision and pattern recognition*. pp. 1625–1634 (2018)
12. Fan, H., Lin, L., Yang, F., Chu, P., Deng, G., Yu, S., Bai, H., Xu, Y., Liao, C., Ling, H.: LaSOT: A high-quality benchmark for large-scale single object tracking. In: *Proceedings of the IEEE/CVF conference on computer vision and pattern recognition*. pp. 5374–5383 (2019)
13. Ghamizi, S., Cordy, M., Papadakis, M., Traon, Y.L.: Adversarial robustness in multi-task learning: Promises and illusions. *arXiv preprint arXiv:2110.15053* (2021)
14. Goodfellow, I.J., Shlens, J., Szegedy, C.: Explaining and harnessing adversarial examples. *arXiv preprint arXiv:1412.6572* (2014)
15. Guo, Q., Feng, W., Zhou, C., Huang, R., Wan, L., Wang, S.: Learning dynamic siamese network for visual object tracking. In: *Proceedings of the IEEE international conference on computer vision*. pp. 1763–1771 (2017)
16. Held, D., Thrun, S., Savarese, S.: Learning to track at 100 fps with deep regression networks. In: *European conference on computer vision*. pp. 749–765. Springer (2016)

17. Ilyas, A., Santurkar, S., Tsipras, D., Engstrom, L., Tran, B., Madry, A.: Adversarial examples are not bugs, they are features. *Advances in neural information processing systems* **32** (2019)
18. Jia, S., Ma, C., Song, Y., Yang, X.: Robust tracking against adversarial attacks. In: *European Conference on Computer Vision*. pp. 69–84. Springer (2020)
19. Jia, S., Song, Y., Ma, C., Yang, X.: Iou attack: Towards temporally coherent black-box adversarial attack for visual object tracking. In: *Proceedings of the IEEE/CVF Conference on Computer Vision and Pattern Recognition*. pp. 6709–6718 (2021)
20. Jia, Y.J., Lu, Y., Shen, J., Chen, Q.A., Chen, H., Zhong, Z., Wei, T.W.: Fooling detection alone is not enough: Adversarial attack against multiple object tracking. In: *International Conference on Learning Representations (ICLR’20)* (2020)
21. Kocabas, M., Karagoz, S., Akbas, E.: Multiposenet: Fast multi-person pose estimation using pose residual network. In: *Proceedings of the European conference on computer vision (ECCV)*. pp. 417–433 (2018)
22. Kong, L., Huang, D., Wang, Y.: Long-term action dependence-based hierarchical deep association for multi-athlete tracking in sports videos. *IEEE Transactions on Image Processing* **29**, 7957–7969 (2020)
23. Kristan, M., Leonardis, A., Matas, J., Felsberg, M., Pflugfelder, R., Kämäräinen, J.K., Danelljan, M., Zajc, L.Č., Lukežič, A., Drbohlav, O., et al.: The eighth visual object tracking vot2020 challenge results. In: *European Conference on Computer Vision*. pp. 547–601. Springer (2020)
24. Kristan, M., Matas, J., Leonardis, A., Felsberg, M., Pflugfelder, R., Kämäräinen, J.K., Chang, H.J., Danelljan, M., Cehovin, L., Lukežič, A., et al.: The ninth visual object tracking vot2021 challenge results. In: *Proceedings of the IEEE/CVF International Conference on Computer Vision*. pp. 2711–2738 (2021)
25. Kristan, M., Matas, J., Leonardis, A., Felsberg, M., Pflugfelder, R., Kamarainen, J.K., Cehovin Zajc, L., Drbohlav, O., Lukežic, A., Berg, A., et al.: The seventh visual object tracking vot2019 challenge results. In: *Proceedings of the IEEE/CVF International Conference on Computer Vision Workshops*. pp. 0–0 (2019)
26. Krizhevsky, A., Sutskever, I., Hinton, G.E.: Imagenet classification with deep convolutional neural networks. *Advances in neural information processing systems* **25** (2012)
27. Li, B., Wu, W., Wang, Q., Zhang, F., Xing, J., Yan, J.: Siamrpn++: Evolution of siamese visual tracking with very deep networks. In: *Proceedings of the IEEE/CVF Conference on Computer Vision and Pattern Recognition*. pp. 4282–4291 (2019)
28. Li, B., Yan, J., Wu, W., Zhu, Z., Hu, X.: High performance visual tracking with siamese region proposal network. In: *Proceedings of the IEEE conference on computer vision and pattern recognition*. pp. 8971–8980 (2018)
29. Liang, Q., Wu, W., Yang, Y., Zhang, R., Peng, Y., Xu, M.: Multi-player tracking for multi-view sports videos with improved k-shortest path algorithm. *Applied Sciences* **10**(3), 864 (2020)
30. Liang, S., Wei, X., Yao, S., Cao, X.: Efficient adversarial attacks for visual object tracking. In: *European Conference on Computer Vision*. pp. 34–50. Springer (2020)
31. Liebel, L., Körner, M.: Multidepth: Single-image depth estimation via multi-task regression and classification. In: *2019 IEEE Intelligent Transportation Systems Conference (ITSC)*. pp. 1440–1447. IEEE (2019)
32. Lin, T.Y., Maire, M., Belongie, S., Hays, J., Perona, P., Ramanan, D., Dollár, P., Zitnick, C.L.: Microsoft coco: Common objects in context. In: Fleet, D., Pajdla, T., Schiele, B., Tuytelaars, T. (eds.) *Computer Vision – ECCV 2014*. pp. 740–755. Springer International Publishing, Cham (2014)

33. Liu, P., Qiu, X., Huang, X.: Adversarial multi-task learning for text classification. arXiv preprint arXiv:1704.05742 (2017)
34. Luo, Y., Tao, D., Geng, B., Xu, C., Maybank, S.J.: Manifold regularized multitask learning for semi-supervised multilabel image classification. *IEEE Transactions on Image Processing* **22**(2), 523–536 (2013)
35. Madry, A., Makelov, A., Schmidt, L., Tsipras, D., Vladu, A.: Towards deep learning models resistant to adversarial attacks. arXiv preprint arXiv:1706.06083 (2017)
36. Mao, C., Gupta, A., Nitin, V., Ray, B., Song, S., Yang, J., Vondrick, C.: Multitask learning strengthens adversarial robustness. In: *Computer Vision - ECCV 2020 - 16th European Conference, Glasgow, UK, August 23–28, 2020, Proceedings, Part II. Lecture Notes in Computer Science*, vol. 12347, pp. 158–174. Springer (2020)
37. Nicolae, M.I., Sinn, M., Tran, M.N., Buesser, B., Rawat, A., Wistuba, M., Zantedeschi, V., Baracaldo, N., Chen, B., Ludwig, H., Molloy, I., Edwards, B.: Adversarial robustness toolbox v1.2.0. CoRR **1807.01069** (2018), <https://arxiv.org/pdf/1807.01069>
38. Ren, S., He, K., Girshick, R., Sun, J.: Faster R-CNN: Towards real-time object detection with region proposal networks. *Advances in neural information processing systems* **28** (2015)
39. Schmidt, L., Santurkar, S., Tsipras, D., Talwar, K., Madry, A.: Adversarially robust generalization requires more data. *Advances in neural information processing systems* **31** (2018)
40. Shuai, B., Berneshawi, A., Li, X., Modolo, D., Tighe, J.: Siammot: Siamese multi-object tracking. In: *Proceedings of the IEEE/CVF conference on computer vision and pattern recognition*. pp. 12372–12382 (2021)
41. Simon-Gabriel, C.J., Ollivier, Y., Bottou, L., Schölkopf, B., Lopez-Paz, D.: First-order adversarial vulnerability of neural networks and input dimension. In: *International Conference on Machine Learning*. pp. 5809–5817. PMLR (2019)
42. Szegedy, C., Zaremba, W., Sutskever, I., Bruna, J., Erhan, D., Goodfellow, I., Fergus, R.: Intriguing properties of neural networks. arXiv preprint arXiv:1312.6199 (2013)
43. Tramèr, F., Kurakin, A., Papernot, N., Goodfellow, I., Boneh, D., McDaniel, P.: Ensemble adversarial training: Attacks and defenses. arXiv preprint arXiv:1705.07204 (2017)
44. Two Six Technologies: ARMORY. <https://github.com/twosixlabs/armory>
45. Wang, X., Shu, X., Zhang, Z., Jiang, B., Wang, Y., Tian, Y., Wu, F.: Towards more flexible and accurate object tracking with natural language: Algorithms and benchmark. In: *Proceedings of the IEEE/CVF Conference on Computer Vision and Pattern Recognition*. pp. 13763–13773 (2021)
46. Wiyatno, R.R., Xu, A.: Physical adversarial textures that fool visual object tracking. In: *Proceedings of the IEEE/CVF International Conference on Computer Vision*. pp. 4822–4831 (2019)
47. Wu, Y., Lim, J., Yang, M.H.: Object tracking benchmark. *IEEE Transactions on Pattern Analysis and Machine Intelligence* **37**(9), 1834–1848 (2015). <https://doi.org/10.1109/TPAMI.2014.2388226>
48. Xu, H., Ma, Y., Liu, H.C., Deb, D., Liu, H., Tang, J.L., Jain, A.K.: Adversarial attacks and defenses in images, graphs and text: A review. *International Journal of Automation and Computing* **17**(2), 151–178 (2020)
49. Xu, K., Zhang, G., Liu, S., Fan, Q., Sun, M., Chen, H., Chen, P.Y., Wang, Y., Lin, X.: Adversarial T-shirt! evading person detectors in a physical world. In: *European conference on computer vision*. pp. 665–681. Springer (2020)

50. Yagi, T., Mangalam, K., Yonetani, R., Sato, Y.: Future person localization in first-person videos. In: Proceedings of the IEEE Conference on Computer Vision and Pattern Recognition. pp. 7593–7602 (2018)
51. Yan, S., Yang, J., Käpylä, J., Zheng, F., Leonardis, A., Kämäräinen, J.K.: Depth-track: Unveiling the power of rgbd tracking. In: Proceedings of the IEEE/CVF International Conference on Computer Vision. pp. 10725–10733 (2021)
52. Yan, Z., Guo, Y., Zhang, C.: Deep defense: Training dnns with improved adversarial robustness. *Advances in Neural Information Processing Systems* **31** (2018)
53. Yao, Y., Xu, M., Wang, Y., Crandall, D.J., Atkins, E.M.: Unsupervised traffic accident detection in first-person videos. In: 2019 IEEE/RSJ International Conference on Intelligent Robots and Systems (IROS). pp. 273–280. IEEE (2019)
54. Ye, S., Bohush, R., Chen, H., Zakharava, I.Y., Ablameyko, S.: Person tracking and reidentification for multicamera indoor video surveillance systems. *Pattern Recognition and Image Analysis* **30**(4), 827–837 (2020)
55. Yu, Y., Xiong, Y., Huang, W., Scott, M.R.: Deformable siamese attention networks for visual object tracking. In: Proceedings of the IEEE/CVF Conference on Computer Vision and Pattern Recognition. pp. 6728–6737 (2020)
56. Zhang, T., Ghanem, B., Liu, S., Ahuja, N.: Robust visual tracking via structured multi-task sparse learning. *International journal of computer vision* **101**(2), 367–383 (2013)
57. Zhang, T., Xu, C., Yang, M.H.: Multi-task correlation particle filter for robust object tracking. In: Proceedings of the IEEE conference on computer vision and pattern recognition. pp. 4335–4343 (2017)
58. Zhang, T., Xu, C., Yang, M.H.: Learning multi-task correlation particle filters for visual tracking. *IEEE transactions on pattern analysis and machine intelligence* **41**(2), 365–378 (2018)
59. Zhang, X., Ye, P., Peng, S., Liu, J., Gong, K., Xiao, G.: Siamft: An rgb-infrared fusion tracking method via fully convolutional siamese networks. *IEEE Access* **7**, 122122–122133 (2019)
60. Zhang, X., Ye, P., Peng, S., Liu, J., Xiao, G.: Dsiammft: An rgb-t fusion tracking method via dynamic siamese networks using multi-layer feature fusion. *Signal Processing: Image Communication* **84**, 115756 (2020)
61. Zhang, Y., Yang, Q.: A survey on multi-task learning. *IEEE Transactions on Knowledge and Data Engineering* (2021)
62. Zhu, X.F., Xu, T., Wu, X.J.: Visual object tracking on multi-modal rgb-d videos: A review. *arXiv preprint arXiv:2201.09207* (2022)
63. Zhu, Z., Wang, Q., Li, B., Wu, W., Yan, J., Hu, W.: Distractor-aware siamese networks for visual object tracking. In: Proceedings of the European conference on computer vision (ECCV). pp. 101–117 (2018)